Electronic Supplementary Material (ESI) for Journal of Materials Chemistry B.

Supplementary Information

Soluble Microneedle Patch with Photothermal and NO-Released Properties for Painless and Precise Treatment of Ischemic Perforator Flaps

Lubing Liu,[a] Qingqing Wang,[b] Huaiwei Liao,[a] Jing Ye,[b] Jinjun Huang,[a] Shisheng Li,[a] Haichuan Peng,[b] Xiang Yu,[b] Huicai Wen,[a] Xiaolei Wang*[b]*

[a] Department of Plastic Surgery, The First Affiliated Hospital of Nanchang University Nanchang, Jiangxi, 330006, China.

[b] The National Engineering Research Center for Bioengineering Drugs and the Technologies: Institute of Translational Medicine, Nanchang University Nanchang, Jiangxi, 330088, China.

*[a] E-mail: whcjxmc@163.com

*[b] Email: wangxiaolei@ncu.edu.cn

* Corresponding authors

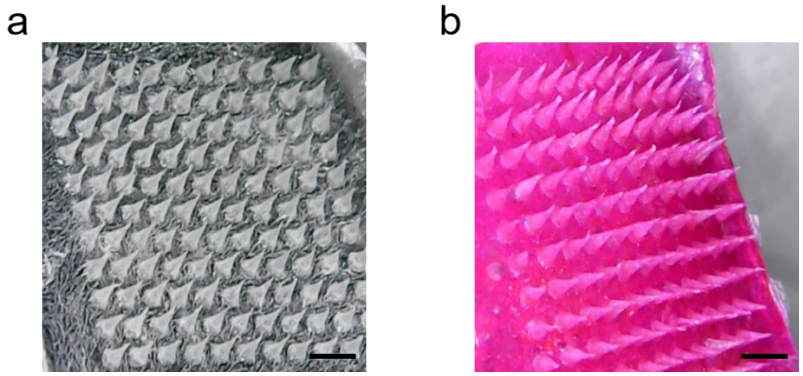

Supplementary Fig. 1 (a-b) Images of the unloaded MN patch (a) and the MN patch stained with Rh B (b) taken by an optical magnifier. (Scale bar = 1 mm).

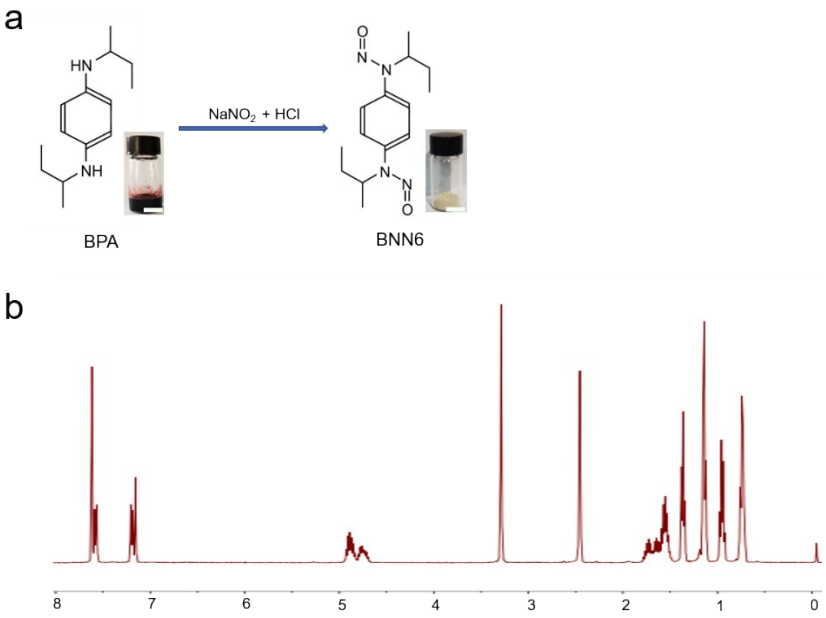

Supplementary Fig. 2 (a) The synthetic route of BNN6. (b) 1H NMR spectrum of BNN6. (Scale bar = 1 cm).

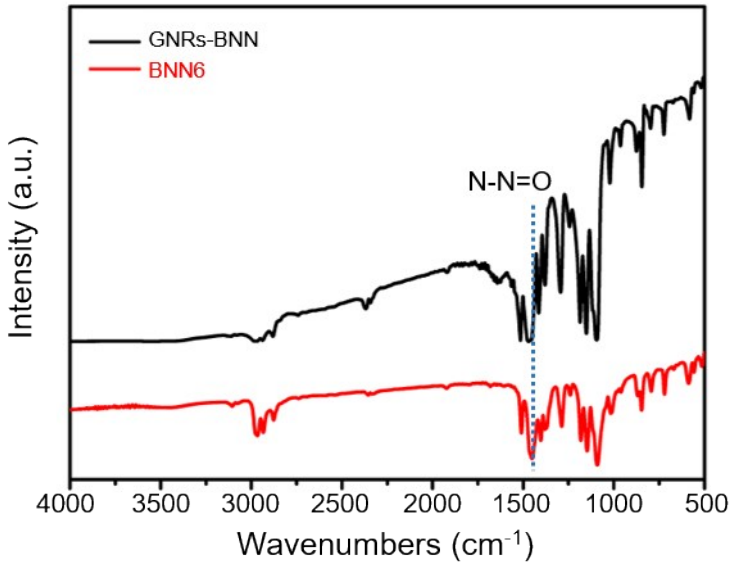

Supplementary Fig. 3 FTIR spectra of GNRs-BNN (black) and BNN6 (red).

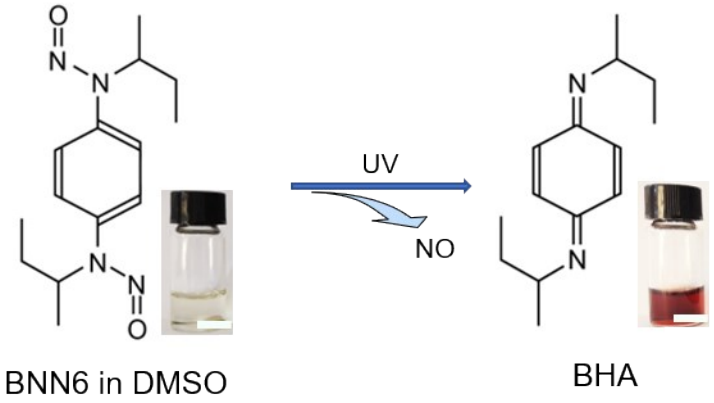

Supplementary Fig. 4 The photochemical degradation of BNN6 to UV light. (Scale bar = 1 cm).

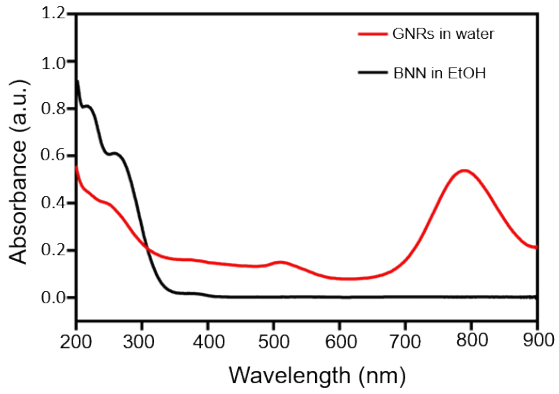

Supplementary Fig. 5 UV-vis spectra of GNRs (red) and BNN (black).

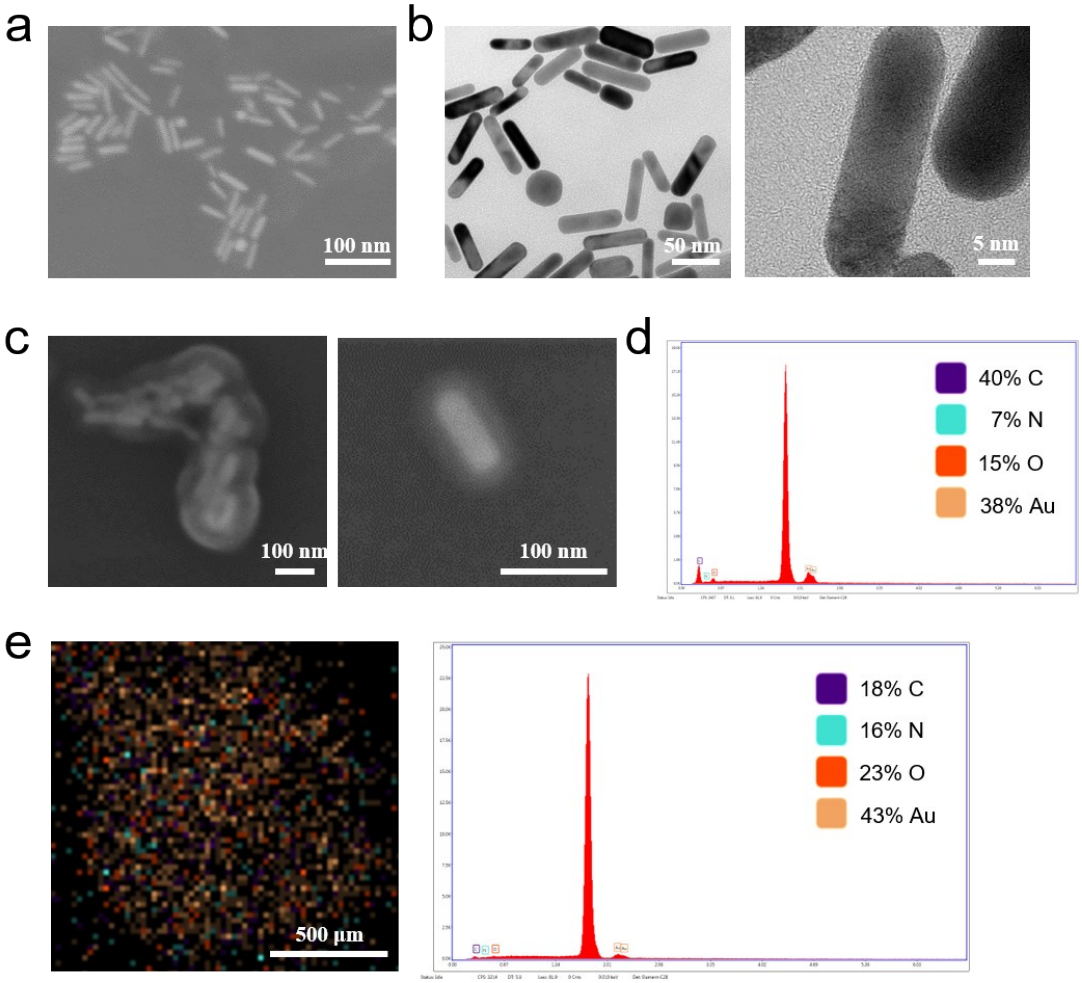

Supplementary Fig. 6 (a-b) SEM image (a) and HR-TEM images (b) of GNRs. (c) SEM images of Tween@GNRs. (d-e) EDS element mapping diagram of Tween@GNRs (d) and GNRs-BNN (e).

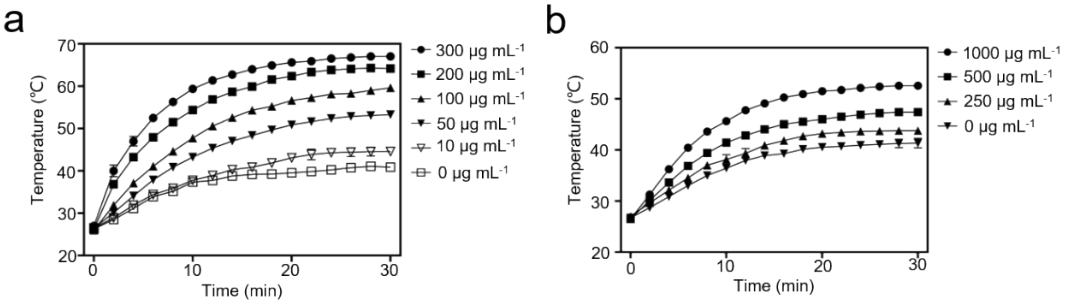

Supplementary Fig. 7 (a) Photothermal performance of GNRs with different concentrations. (b) Photothermal performance of GNRs-BNN with different concentrations. Data are mean ± SD. (n = 3).

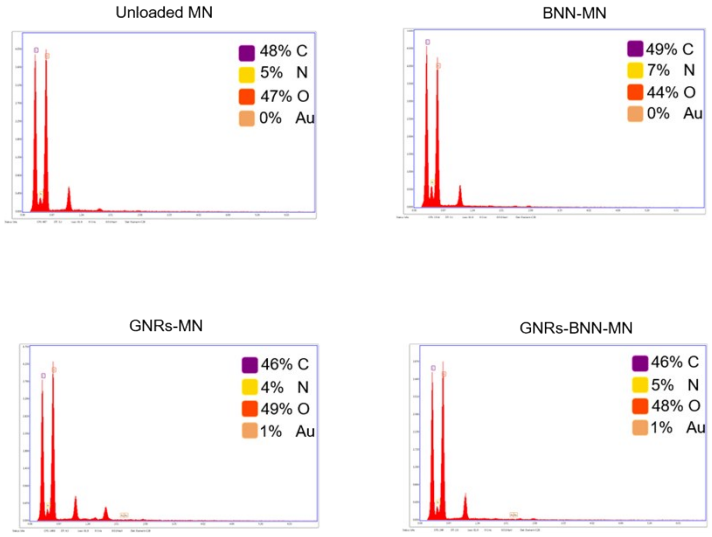

Supplementary Fig. 8 Energy spectrum analysis of four kinds of microneedle patches.

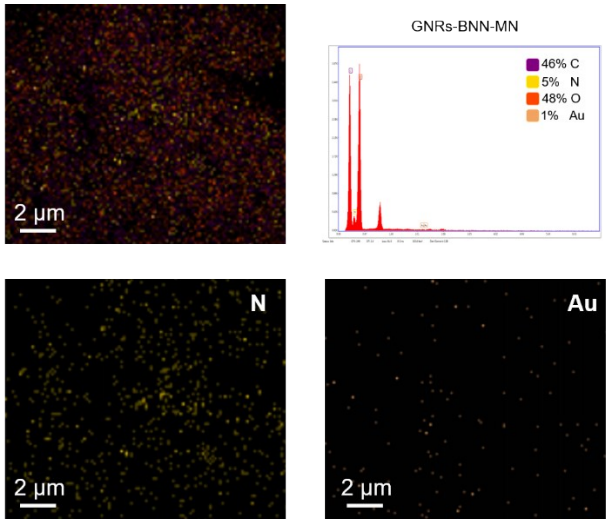

Supplementary Fig. 9 Energy spectrum analysis of four kinds of microneedle patches.

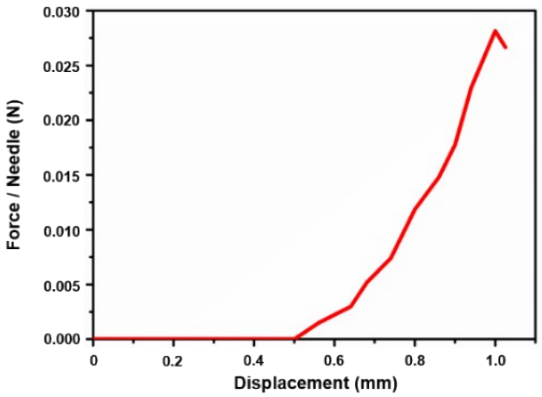

Supplementary Fig. 10 Mechanical behaviors of the GNRs-BNN-MN.

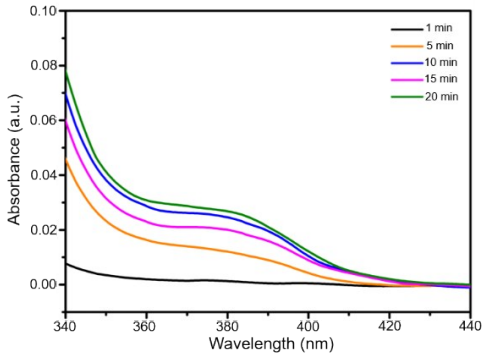

Supplementary Fig. 11 The release of the GNRs-BNN drug from a MN patch.

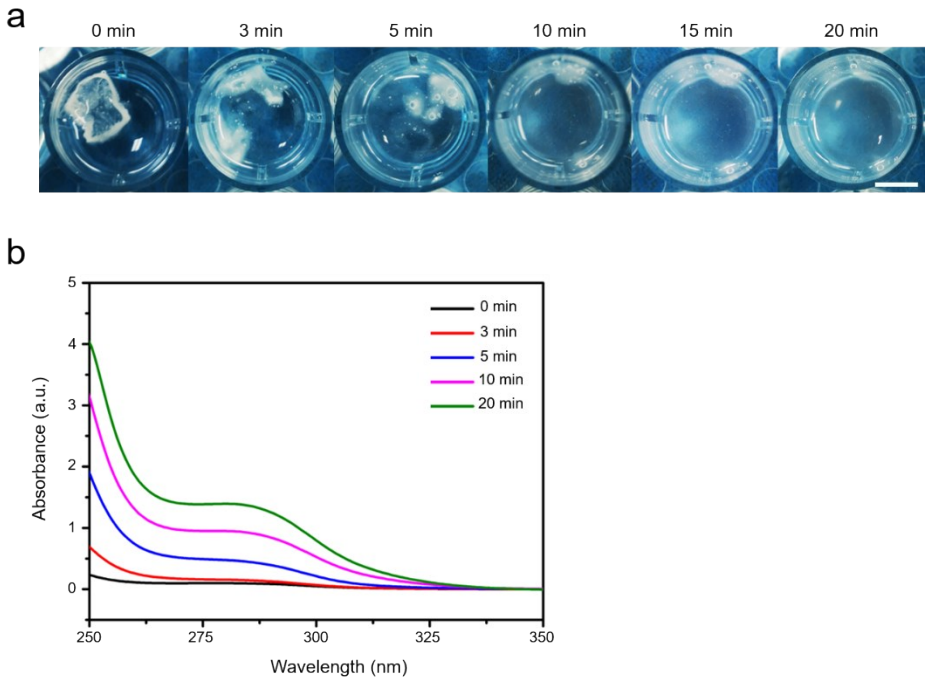

Supplementary Fig. 12 (a) Optical pictures of dissolving microneedles. (Scale bar = 1 cm). (b) Variations of the UV absorption peak of m-HA in the dissolving solution.

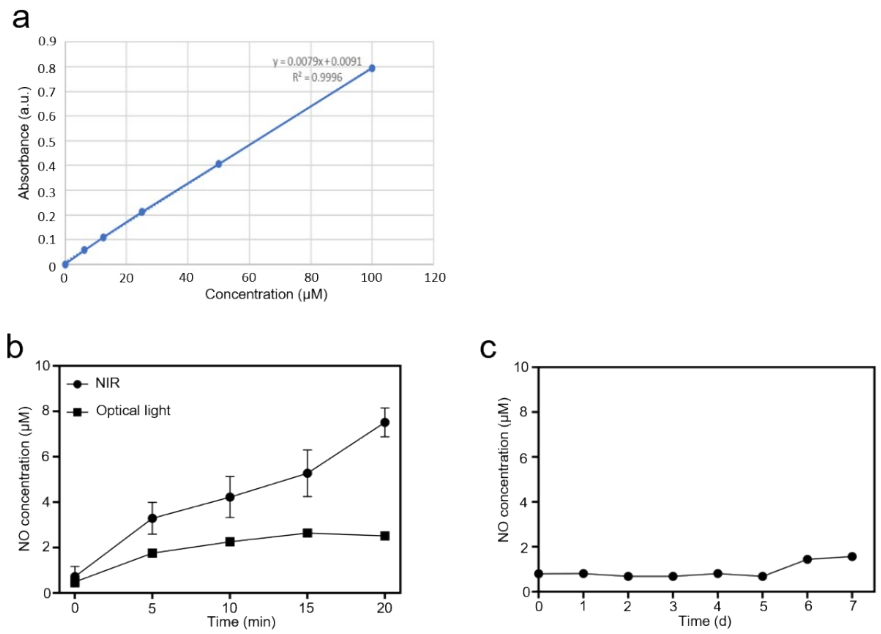

Supplementary Fig. 13 (a) A standard curve for calculation of NO concentrations. (b) NO release under NIR and the optical light irradiation. (c) NO release in a dark environment for 7 days. Data are mean ± SD. (n = 3).

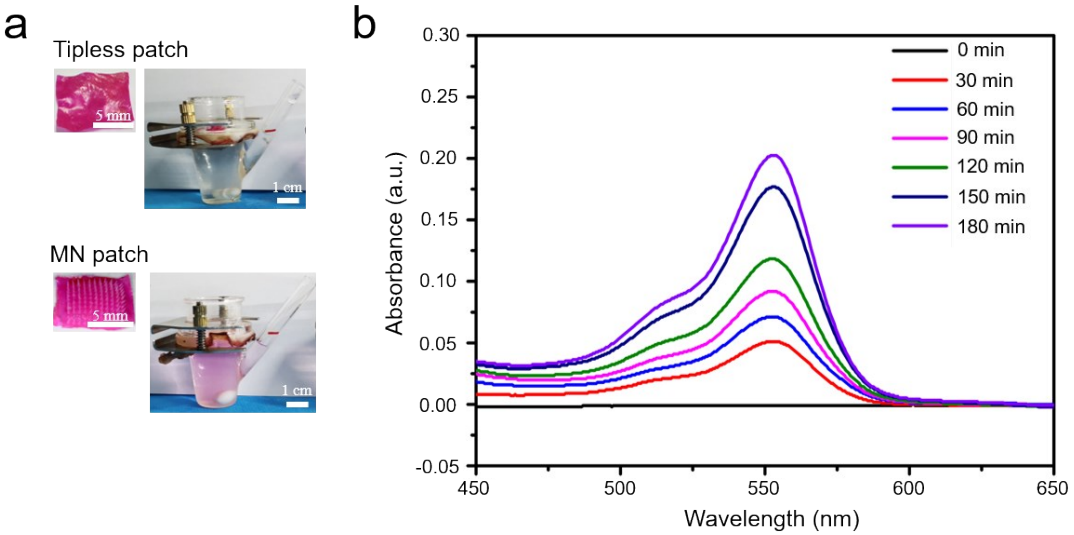

Supplementary Fig. 14 (a) The color change of the solution in the franz cells of tipless patch group and MN patch group. (b) Transdermal Rh B through a MN patch over time.

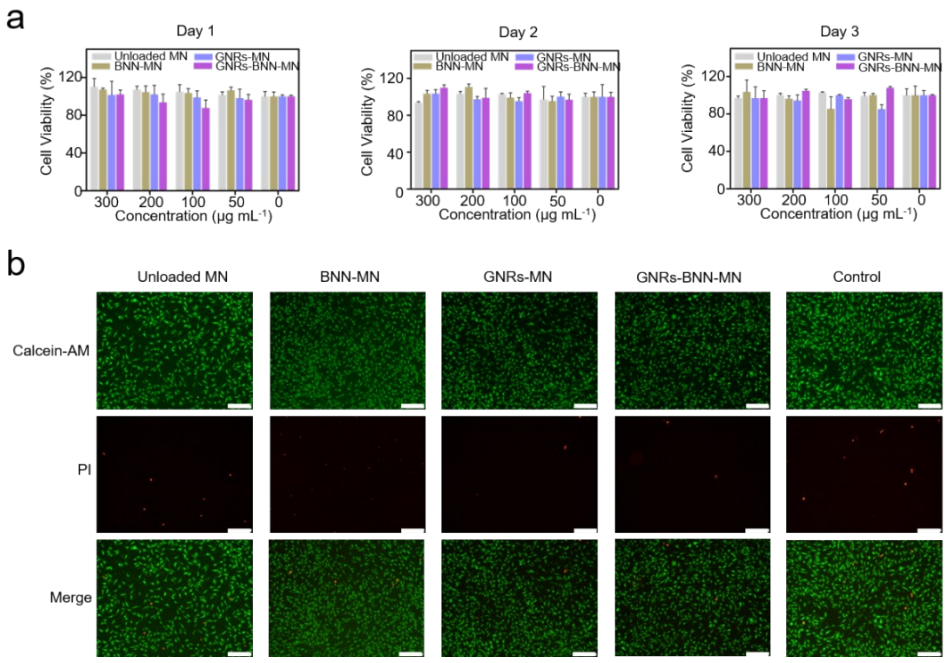

Supplementary Fig. 15 (a) The cell viability of L929 cultured with different MN patches for 1, 2 and 3 days. (b) Live-dead staining assay. Live and dead cells were stained with green and red fluorescent stains. (Scale bar = 100 μm). Data are mean ± SD. (n = 3).

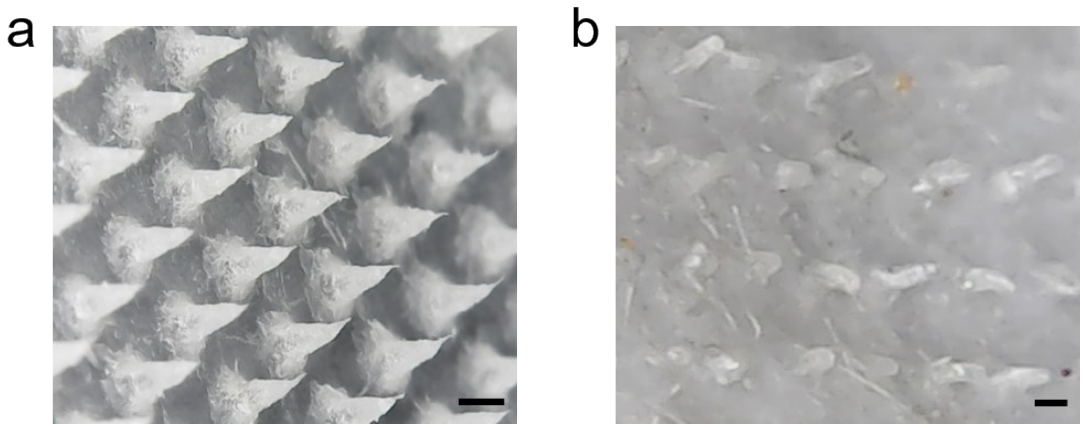

Supplementary Fig. 16 (a-b) Images of the MN patch before (a) and after (b) application taken by an optical magnifier. (Scale bar = 300 μm).

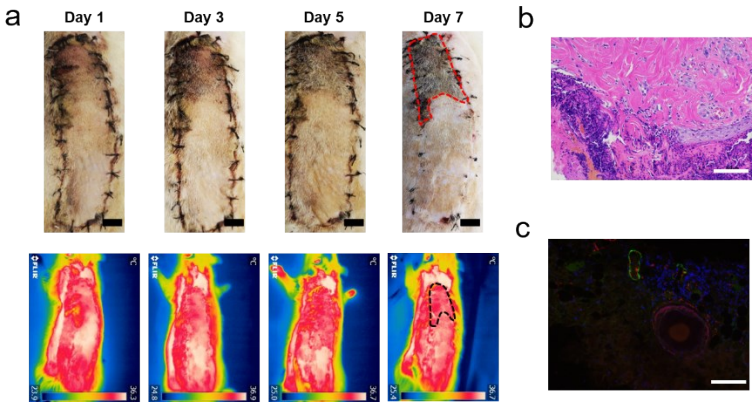

Supplementary Fig. 17 GNRs-BNN-MN group in animal experiment. (a) Photographic images of the skin flaps and the thermal imaging captured real time temperature of skin surface after operation. The red circle represented the necrotic area and the black circle represented the low temperature area. (Scale bar = 1 cm). (b) H&E staining. (Scale bar = 100 μm). (c) Immunohistochemical staining. (Scale bar = 100 μm).

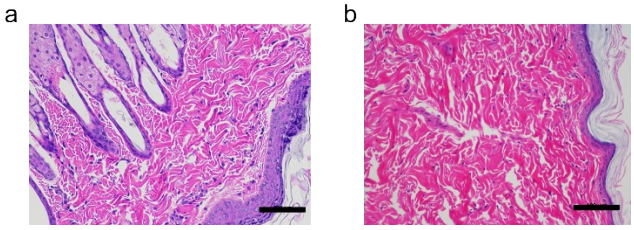

Supplementary Fig. 18 H&E staining showing the normal skin (a) and the skin treated by the MN patch under NIR irradiation (b).

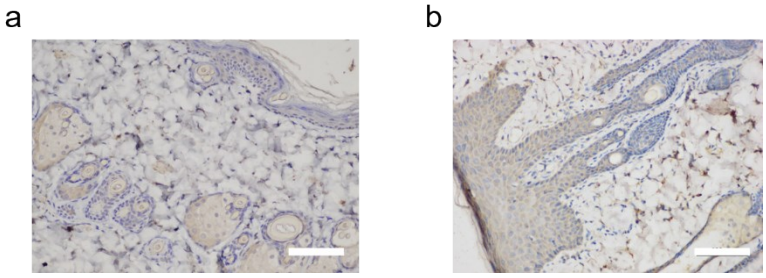

Supplementary Fig. 19 Immunostaining of CD68 in normal skin (a) and in the skin treated by the MN patch (b). (Scale bar = 100 μm).

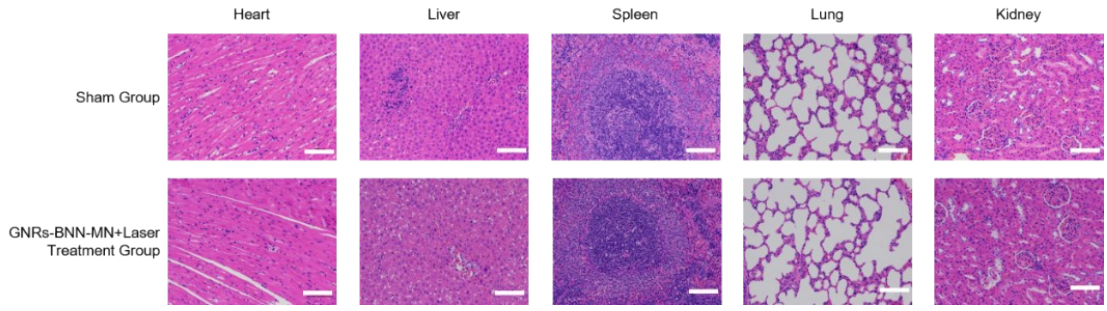

Supplementary Fig. 20 H&E-stained tissue sections from major organs in rats 7 days after the operation. (Scale bar = 100 μm).